Partonic Scattering Cross Sections in the QCD Medium

Jörg Ruppert, Gouranga C. Nayak *, Dennis D. Dietrich, Horst Stöcker, and Walter Greiner
Institut für Theoretische Physik, J. W. Goethe-Universität, 60054 Frankfurt am Main, Germany

Abstract

A medium modified gluon propagator is used to evaluate the scattering cross section for the process $gg \to gg$ in the QCD medium by performing an explicit sum over the polarizations of the gluons. We incorporate a magnetic sreening mass from a non - perturbative study. It is shown that the medium modified cross section is finite, divergence free, and is independent of any ad-hoc momentum transfer cut-off parameters. The medium modified finite cross sections are necessary for a realistic investigation of the production and equilibration of the minijet plasma expected at RHIC and LHC.

PACS: 12.38.Mh; 14.70.Dj; 12.38.Bx; 11.10.Wx

*present address: T-8, Theoretical Division, Los Alamos National Laboratory, Los Alamos, NM 87545, USA

A lot of research is undertaken to detect a new state of matter, known as the quark-gluon plasma (QGP) which is believed to have existed in the early stage of the universe, $\sim 10^{-4}$ seconds after the big bang. [1,2] Lattice QCD calculations indicate that this deconfined state of quark gluon matter exists at high temperatures ($\sim 200\ MeV$) or high energy densities ($\sim 2\ GeV/fm^3$) [3]. The relativistic heavy-ion colliders RHIC (Au-Au collisions at $\sqrt{s} = 200\ A\ GeV$) and LHC (Pb-Pb collisions at $\sqrt{s} = 5.5\ A\ TeV$) offer the unique opportunity to study the production of this state of matter in the laboratory [1]. Perturbative QCD (pQCD) estimates that the energy density of jets and minijets produced in these collisions could be larger than about 50 and 1000 GeV/fm^3 at RHIC and LHC respectively [4,5]. However, even if the attained energy density is sufficient to form a quark-gluon plasma, it is not at all clear whether the parton medium will equilibrate and form a thermalized quark-gluon plasma before hadronization. Evidence for the formation of a QGP at RHIC and LHC can only be established if various proposed signatures have been examined experimentally. The most prominent signatures suggested so far are J/Ψ suppression [6], strangeness enhancement [7], and dilepton and direct photon production [8–11]. A quantitative calculation of these predicted signatures will be difficult to achieve for the situations found at RHIC and LHC. One main uncertainty originates from the absence of a reliable study of the space-time evolution of the parton distributions in these experiments. An investigation of this evolution will determine the equilibration times and the time evolution of all other local and global quantities such as energy densities, number densities, and temperatures of the SU(4)-flavour components of the quark-gluon plasma.

The space-time evolution of the QGP during an ultra-relativistic heavy-ion collision might proceed through different stages such as: 1) the pre-equilibrium, 2) the equilibrium, and 3) the hadronization stage. During the equilibrium stage, hydrodynamics can be used to describe the dynamics of the QGP. However, both the pre-equilibrium and the hadronization stages have to be studied in more detail in order to see whether either partons or hadrons equilibrate or not. The first stage starts just after the initial nuclear collisions, where many hard, semihard, and soft partons are produced. The hard and semihard partons (jets and minijets) formed at RHIC and LHC can be desribed by using pQCD [4,5,12]), and soft gluons may be described by the creation of a coherent chromofield [13–17]. For the sake of simplicity, we restrict our investigation to jets and minijets only. The equilibration of a minijet plasma can be studied by solving the relativistic transport equations with binary and secondary parton-parton collisions taken into account [18]:

$$p^\mu \partial_\mu f(x,p) \ = \ C(x,p). \tag{1}$$

In equation (1)

$$C(x,p) \ = \ \int \frac{d^3p_2}{(2\pi)^3 p_2^0} \frac{d^3p_3}{(2\pi)^3 p_3^0} \frac{d^3p_4}{(2\pi)^3 p_4^0} \ |M(pp_2 \to p_3p_4)|^2 \ [f(x,p_3)f(x,p_4) - f(x,p)f(x,p_2)] \tag{2}$$

is the collision term for the 2 body partonic scattering process $pp_2 \to p_3p_4$. The collisions among the partons determine how the QGP reaches equilibrium. So, the investigation of the 2-body collision cross section in the non-equilibrated medium is of great importance for the understanding of the minijet plasma evolution at RHIC and LHC. The different partonic

scattering processes which have to be considered are e.g. $gg \to gg$, $qq \to qq$, $q\bar{q} \to q\bar{q}$ etc. and in more detailed studies also higher order processes like $gg \to ggg$ might have to be taken into account. Most probably, the dominant part of the minijets consists of gluons. Hence we consider collisions of the type: $gg \to gg$. The differential cross section for this process is given by:

$$\frac{d\sigma}{dt} \;=\; \frac{9\pi\alpha_s^2}{2s^2}\,[3 - \frac{ut}{s^2} - \frac{us}{t^2} - \frac{st}{u^2}], \tag{3}$$

where $s = (q_1 + q_2)^2 = (q_3 + q_4)^2$, $t = (q_1 - q_4)^2 = (q_2 - q_3)^2$, and $u = (q_1 - q_3)^2 = (q_2 - q_4)^2$ are the Mandelstam variables of the partons. For real gluons, they are related by

$$t \;=\; -\frac{s}{2}\,[1 - \cos\theta_{\rm cm}] \quad \text{and} \quad u \;=\; -\frac{s}{2}\,[1 + \cos\theta_{\rm cm}], \tag{4}$$

where $\theta_{\rm cm}$ is the center of mass scattering angle, which goes from $0 \to \frac{\pi}{2}$ for identical particles in the final state. If $|M(s,u,t)|^2$ is put from Eq.(3) into Eq.(2), a divergence emerges in the collision term at small angle ($\theta_{\rm cm} \to 0$), which corresponds to collisions with small momentum transfer ($t \to 0$). Hence, to obtain a finite collision term, one is forced to put a minimum momentum transfer by hand, as it is done in the parton cascade model [19]. The plasma evolution and the determination of all the signatures then crucially depend on the choice of this momentum cut-off parameter.

The equilibration time and equilibration process can be studied by using a collision term in the relaxation-time approximation for the transport equation [20,21,4]:

$$C(x,p) \;=\; p^\mu u_\mu\,[f(x,p) - f_{eq}(x,p)]/\tau_c(\tau), \tag{5}$$

where $\tau_c(\tau)$ is the time dependent relaxation time and $f_{eq} = (e^{p^\mu u_\mu/T(\tau)} - 1)^{-1}$ is the Bose-Einstein distribution function. u_μ represents the flow velocity. The time dependent relaxation time $\tau_c(\tau)$ can be determined from the transport cross section (σ_{tr}) and the number density (n) of the plasma via the relation [4,20,22]:

$$\tau_c(\tau) \;=\; \frac{1}{\sigma_{tr}(\tau)\; n(\tau)}. \tag{6}$$

Here, the time dependent number density is determined from the non-equilibrium distribution function via:

$$n(\tau) \;=\; \int \frac{d^3p}{(2\pi)^3 p^0}\; p^\mu u_\mu\; f(x,p) \tag{7}$$

and the transport cross section for the $gg \to gg$ collisions is given by:

$$\sigma_t(\tau) \;=\; \int_{-\frac{s}{2}}^{0} dt\; \frac{d\sigma^{2\to2}}{dt}\; \sin^2\theta_{\rm cm} \;=\; \int_{-\frac{s}{2}}^{0} dt\; \frac{1}{16\pi s^2}\; |M(s,t,u)|^2\; \frac{4tu}{s^2}. \tag{8}$$

Hence, whether one uses Eq.(2) or (5) as the collision term, one always encounters the divergence in the limit $t \to 0$.

This divergence is inescapable as long as we are considering the propagator in the vacuum. As the equilibration of the quark-gluon plasma crucially depends on the cut-off used

to remove these divergences [19], it is essential to incorporate the medium effects to obtain finite and cut-off independent partonic scattering cross-sections in the QCD medium. Here, one should therefore use the the medium modified propagator instead of the vacuum propagator. In this paper, we evaluate and analyze the matrix element squared, total cross section, and transport cross section for the process $gg \to gg$ by using the medium modified propagator performing an explicit sum over the polarizations of the physical gluons. This analysis is important to study the evolution of the QGP because the divergence is removed automatically and cut-off independently.

In this paper we choose the medium modified gluon propagator in the covariant gauge. It can be split into the longitudinal and transverse parts [23,24]:

$$\Delta^{\mu\nu}(K) = \frac{P_T^{\mu\nu}}{-K^2 + \Pi_T} + \frac{P_L^{\mu\nu}}{-K^2 + \Pi_L} + (\alpha - 1)\frac{K^\mu K^\nu}{K^4} \tag{9}$$

where α is the gauge fixing parameter. $P_T^{\mu\nu}$ and $P_L^{\mu\nu}$ are longitudinal and transverse tensors given by:

$$\begin{aligned} P_L^{\mu\nu} &= \frac{-(\omega K^\mu - K^2 U^\mu)(\omega K^\nu - K^2 U^\nu)}{K^2 k^2} \\ P_T^{\mu\nu} &= \tilde{g}^{\mu\nu} + \frac{\tilde{K}^\mu \tilde{K}^\mu}{k^2}, \end{aligned} \tag{10}$$

$\tilde{g}_{\mu\nu} = g_{\mu\nu} - U_\mu U_\nu$ with U_μ being the flow velocity. The quantity $\omega = K \cdot U$ is interpreted as the Lorentz-invariant energy and $k = \sqrt{-\tilde{K}_\mu \tilde{K}^\mu}$ with $\tilde{K}_\mu = K_\mu - U_\mu(K \cdot U)$ as the three momentum of the virtual boson. In the local rest frame ($U = (1, \vec{0})$), ω and $\vec{k}$ are its energy and momentum. The expressions for Π_L and Π_T in the high temperature expansion are derived by perturbative methods in [23]:

$$\begin{aligned} \Pi_L &= m_D^2(1 - x^2)[1 - \frac{x}{2}\log|\frac{1+x}{1-x}| + i\frac{\pi}{2}x] \\ \Pi_T &= m_D^2[\frac{x^2}{2} + \frac{x}{4}(1 - x^2)\log|\frac{1+x}{1-x}| - i\frac{\pi}{4}x(1 - x^2)], \end{aligned} \tag{11}$$

where $x = \frac{\omega}{k}$ and $m_D = g^2 T^2$. The t-channel matrix element for the process $gg \to gg$ in the medium is given by:

$$M = g^2 f_{aed} f_{ebc} \epsilon_1^\lambda \epsilon_4^\sigma V^{\lambda\tau\sigma}(-q_1, q_1 - q_4, q_4) \Delta_{\tau'\tau}(q_1 - q_4) V^{\tau'\mu\nu}(q_2 - q_3, -q_2, q_3) \epsilon_2^\mu \epsilon_3^\nu, \tag{12}$$

where $V^{\mu\lambda\nu}(p_1, p_2, p_3) = [(p_1 - p_2)^\nu g^{\mu\lambda} + (p_2 - p_3)^\mu g^{\lambda\nu} + (p_3 - p_1)^\lambda g^{\mu\nu}]$ is the three gluon vertex, $\epsilon^\mu(p)$ are the polarization vectors of the gluons and $\Delta^{\mu\nu}(k)$ is the medium modified gluon propagator given by Eq. (9).

To sum over initial and final spins of the gluons in the matrix element squared, we use the appropriate projection operators for the transverse polarization states of the gluons [25,26]:

$$\begin{aligned} &\sum_{\text{spins}} \epsilon_1^\lambda \epsilon_1^{*\lambda'} = -g^{\lambda\lambda'} + \frac{2(q_1^\lambda q_2^{\lambda'} + q_1^{\lambda'} q_2^\lambda)}{(q_1 + q_2)^2} \quad , \qquad \sum_{\text{spins}} \epsilon_2^\mu \epsilon_2^{*\mu'} = -g^{\mu\mu'} + \frac{2(q_1^\mu q_2^{\mu'} + q_1^{\mu'} q_2^\mu)}{(q_1 + q_2)^2} \\ &\sum_{\text{spins}} \epsilon_3^\nu \epsilon_3^{*\nu'} = -g^{\nu\nu'} + \frac{2(q_3^\nu q_4^{\nu'} + q_3^{\nu'} q_4^\nu)}{(q_3 + q_4)^2} \quad , \text{ and } \sum_{\text{spins}} \epsilon_4^\sigma \epsilon_4^{*\sigma'} = -g^{\sigma\sigma'}. \end{aligned} \tag{13}$$

After summing over the final and averaging over the initial spins and color, we obtain (in Feynman gauge):

$$|M|^2_{\text{medium}} = \frac{A}{s^3(t-(t_{\rm v}\cdot U)^2)^2(\Pi_L - t)(\bar{\Pi}_L - t)} - \frac{B}{s^3(t-(t_{\rm v}\cdot U)^2)^2(\Pi_T - t)(\bar{\Pi}_L - t)} - \frac{B}{s^3(t-(t_{\rm v}\cdot U)^2)^2(\Pi_L - t)(\bar{\Pi}_T - t)} + \frac{C}{s^3(t-(t_{\rm v}\cdot U)^2)^2(\Pi_T - t)(\bar{\Pi}_T - t)}, \quad (14)$$

where A, B, C are:

$$\begin{aligned} A = \frac{9}{8}t^2 g^4 \{ & (s^2\ [(s_{\rm v}\cdot U - u_{\rm v}\cdot U)^2 + 4(t-(t_{\rm v}\cdot U)^2)] + 2ts\ [2t + (u_{\rm v}\cdot U)^2 - (s_{\rm v}\cdot U)^2 - 2(t_{\rm v}\cdot U)^2] + \\ & 2t^2\ [(u_{\rm v}\cdot U)^2 + 2(u_{\rm v}\cdot U)(s_{\rm v}\cdot U) - (s_{\rm v}\cdot U)^2]) \times (t\ [2t + (u_{\rm v}\cdot U)^2 - 2(t_{\rm v}\cdot U)^2 - (s_{\rm v}\cdot U)^2] \\ & + s\ [(s_{\rm v}\cdot U + u_{\rm v}\cdot U)^2 + 3(t-(t_{\rm v}\cdot U)^2)])\} \end{aligned} \quad (15)$$

$$\begin{aligned} B = \frac{9}{8}tg^4 \{ & 2s^4\ [t-(t_{\rm v}\cdot U)^2][(u_{\rm v}\cdot U)^2 - (s_{\rm v}\cdot U)^2] + s^3 t\ [(s_{\rm v}\cdot U)^4 + 2(t-(t_{\rm v}\cdot U)^2 - (u_{\rm v}\cdot U)^2) \\ & (s_{\rm v}\cdot U)^2 + 2(t-(t_{\rm v}\cdot U)^2)(u_{\rm v}\cdot U)(s_{\rm v}\cdot U) + (u_{\rm v}\cdot U)^2(4t + (u_{\rm v}\cdot U)^2 - 4(t_{\rm v}\cdot U)^2)] \\ & + s^2t^2[-3(s_{\rm v}\cdot U)^4 - 2(u_{\rm v}\cdot U)(s_{\rm v}\cdot U)^3 + 2(t-(t_{\rm v}\cdot U)^2)(s_{\rm v}\cdot U)^2 + (u_{\rm v}\cdot U)(-5(t_{\rm v}\cdot U)^2 \\ & + 2(u_{\rm v}\cdot U)^2 + 5t)(s_{\rm v}\cdot U) + (u_{\rm v}\cdot U)^2(-5(t_{\rm v}\cdot U)^2 + 3(u_{\rm v}\cdot U)^2 + 5t)] + 2st^3(u_{\rm v}\cdot U) \\ & [2(u_{\rm v}\cdot U)(s_{\rm v}\cdot U)^2 + 4(-(t_{\rm v}\cdot U)^2 + (u_{\rm v}\cdot U)^2 + t)(s_{\rm v}\cdot U) + (u_{\rm v}\cdot U)(-3(t_{\rm v}\cdot U)^2 + \\ & 2(u_{\rm v}\cdot U)^2 + 3t)] + 2t^4\ [s_{\rm v}\cdot U + u_{\rm v}\cdot U] \times [(s_{\rm v}\cdot U)^3 - 3u_{\rm v}\cdot U(s_{\rm v}\cdot U)^2 \\ & + (u_{\rm v}\cdot U)^2(s_{\rm v}\cdot U) + (u_{\rm v}\cdot U)(t + (u_{\rm v}\cdot U)^2 - (t_{\rm v}\cdot U)^2)]\} \end{aligned} \quad (16)$$

$$\begin{aligned} C = \frac{9}{8}g^4 \{ & 4s^5\ [t-(t_{\rm v}\cdot U)^2]^2 + 4s^4 t\ [t-(t_{\rm v}\cdot U)^2]\ [t - (s_{\rm v}\cdot U)^2 - (t_{\rm v}\cdot U)^2 + (u_{\rm v}\cdot U)^2] \\ & + s^3t^2\ [(s_{\rm v}\cdot U)^4 + (3(t_{\rm v}\cdot U)^2 - 2(u_{\rm v}\cdot U)^2 - 3t)(s_{\rm v}\cdot U)^2 + 2((t-(t_{\rm v}\cdot U)^2)(u_{\rm v}\cdot U)(s_{\rm v}\cdot U) \\ & (u_{\rm v}\cdot U)^4 + 4(t-(t_{\rm v}\cdot U)^2)^2 + (t-(t_{\rm v}\cdot U)^2)(u_{\rm v}\cdot U)^2)] + s^2t^3\ [-3(s_{\rm v}\cdot U)^4 \\ & -2(u_{\rm v}\cdot U)(s_{\rm v}\cdot U)^3 + 8(t-(t_{\rm v}\cdot U)^2)(s_{\rm v}\cdot U)^2 + 2u_{\rm v}\cdot U(-3(t_{\rm v}\cdot U)^2 + (u_{\rm v}\cdot U)^2 + 3t)s_{\rm v}\cdot U \\ & +3(u_{\rm v}\cdot U)^4 + 7(t-(t_{\rm v}\cdot U)^2)^2 - 6(t - t_{\rm v}\cdot U^2)(u_{\rm v}\cdot U)^2)] + 2st^4\ [2(u_{\rm v}\cdot U)^4 + 4(s_{\rm v}\cdot U)(u_{\rm v}\cdot U)^3 \\ & +(2(s_{\rm v}\cdot U)^2 + (t_{\rm v}\cdot U)^2 - t)(u_{\rm v}\cdot U)^2 + 2s_{\rm v}\cdot U(t-(t_{\rm v}\cdot U)^2)u_{\rm v}\cdot U + (t-(t_{\rm v}\cdot U)^2)(7(s_{\rm v}\cdot U)^2 \\ & -(t_{\rm v}\cdot U)^2 + t)] + 2t^5\ [(s_{\rm v}\cdot U)^4 - 2u_{\rm v}\cdot U(s_{\rm v}\cdot U)^3 + 2(-(t_{\rm v}\cdot U)^2 - (u_{\rm v}\cdot U)^2 + t)(s_{\rm v}\cdot U)^2 \\ & +2u_{\rm v}\cdot U((t_{\rm v}\cdot U)^2 + (u_{\rm v}\cdot U)^2 - t)s_{\rm v}\cdot U + (u_{\rm v}\cdot U)^4 - (t-(t_{\rm v}\cdot U)^2)^2]\}. \end{aligned} \quad (17)$$

U is the flow velocity and $s_{\rm v},\ t_{\rm v},\ u_{\rm v}$ are defined as follows

$$s^\mu_{\rm v} = (q_1+q_2)^\mu = (q_3+q_4)^\mu,\ t^\mu_{\rm v} = (q_3-q_2)^\mu = (q_1-q_4)^\mu,\ u^\mu_{\rm v} = (q_1-q_3)^\mu = (q_4-q_2)^\mu. \quad (18)$$

The Mandelstam variables of the partons are just given as:

$$s_v\cdot s_v = s,\ t_v\cdot t_v = t,\ u_v\cdot u_v = u. \quad (19)$$

Eq. (14) together with Eqs. (15) to (17) show the general expression for the t-channel matrix element squared of the scattering process $gg \to gg$ in the medium. As this is a

rather lengthy expression, we analyze the behavior of this scattering term in the local rest frame of the fluid $U = (1, \vec{0})$. In the center of mass frame of the parton-parton collision Eq. (14) becomes:

$$(\frac{d\sigma}{dt})_{\rm medium} = \frac{9\pi\alpha^2}{8}\{\frac{(s^2+2ts+2t^2)^2}{s^4(\Pi_L - t)(\bar{\Pi}_L - t)} + \frac{(s+t)(s^2-2t^2)}{s^3(\Pi_T - t)(\bar{\Pi}_L - t)} + \frac{(s+t)(s^2-2t^2)}{s^3(\Pi_L - t)(\bar{\Pi}_T - t)} + \frac{(s+t)(s^4-3ts^3+15t^2s^2+8t^3s-2t^4)}{s^5(\Pi_T - t)(\bar{\Pi}_T - t)}\}. \quad (20)$$

Using the in-vacuum gluon propagator and repeating the above procedure one finds for the t-channel process:

$$(\frac{d\sigma}{dt})_{\rm vacuum} = \frac{9\pi\alpha^2}{8}\frac{4s^5+4ts^4+16t^2s^3+27t^3s^2+10t^4s-2t^5}{s^5t^2}. \quad (21)$$

It can be verified that for $\Pi_L = 0$ and $\Pi_T = 0$ Eq.(20) reduces to Eq.(21). In the limit $t \to 0$ the dominant divergent part of Eq.(21) is given by:

$$(\frac{d\sigma}{dt})_{\rm lead.vacuum} = \frac{9\pi\alpha^2}{2t^2}. \quad (22)$$

This divergence can be removed by introducing a screening mass m_D by hand [21,4]:

$$(\frac{d\sigma}{dt})_{\rm lead.cut-off} = \frac{9\pi\alpha^2}{2(t-m_D^2)^2}. \quad (23)$$

The introduction of the Debye screening mass (the longitudinal part of the self energy) in the above formula leads to a screening of the long range electric field but not of the magnetic field. However, Eq. (20) can be used to screen both the electric and magnetic (beyond one loop in self energy evaluation) part simultaneously. For a comparison with Eq. (23) we extract the terms quadratic in t in the denominator of Eq. (20):

$$(\frac{d\sigma}{dt})_{\rm lead.medium} = \frac{9\pi\alpha^2}{8}\{\frac{1}{(\Pi_L - t)(\bar{\Pi}_L - t)} + \frac{1}{(\Pi_T - t)(\bar{\Pi}_L - t)} + \frac{1}{(\Pi_L - t)(\bar{\Pi}_T - t)} + \frac{1}{(\Pi_L - t)(\bar{\Pi}_T - t)}\}. \quad (24)$$

This equation gives the principal contribution to the total cross section (see below). Hence, this expression can be used for all practical purposes during the evolution of the plasma. In the situation we are considering, it can be easily checked that in the leading order $\Pi_L = m_D^2 = g^2T^2$ and $\Pi_T = 0$. This suggests that even if we consider Eq.(24), the magnetic part is still not screened as long as we use the perturbative expression of the self-energies in the leading order. In this study, the logarithmic singularity in the transverse part of the total cross section is removed by introducing a non-perturbative magnetic screening mass $m_{\rm mag}^2 = \frac{3}{2}(0.255g^2T)^2$ taken from [27,28]. With these self energies Eq.(24) can be integrated to obtain the total cross section:

$$(\sigma_{\rm tot})_{\rm lead.medium} = \int_{-\frac{s}{2}}^{0} dt\ (\frac{d\sigma}{dt})_{\rm lead.medium} = \frac{9\pi\alpha^2}{8}(\frac{s}{\Pi_L(s+2\Pi_L)} + \frac{1}{\Pi_T} + 2\frac{\ln(\frac{s}{\Pi_L}+2) - \ln(\frac{s}{\Pi_T}+2)}{\Pi_T - \Pi_L} - \frac{2}{s+2\Pi_T}), \quad (25)$$

and the transport cross section:

$$
\begin{aligned}
(\sigma_{\rm tr})_{\rm lead.medium} &= \int_{-\frac{s}{2}}^{0} dt\ (\frac{d\sigma}{dt})_{\rm lead.medium}\ \frac{4ut}{s^2} = \\
&= \frac{9\pi\alpha^2}{4}\{2\frac{\ln(\frac{s}{2\Pi_L}+1)+\ln(\frac{s}{2\Pi_T}+1)}{s} - \frac{4}{s} - \frac{1}{s+2\Pi_L} - \frac{1}{s+2\Pi_T} \\
&+ \frac{8\ln(\frac{s}{2\Pi_L}+1)\Pi_L^2 - 2(s(1-2\ln(\frac{s}{2\Pi_L}+1)) + 2(\ln(\frac{s}{2\Pi_L}+1)-\ln(\frac{s}{2\Pi_T}+1))\Pi_T)\Pi_L}{s^2(\Pi_L-\Pi_T)} \\
&+ \frac{2\Pi_T(s(1-2\ln(\frac{s}{2\Pi_T}+1)) - 4\ln(\frac{s}{2\Pi_T}+1)\Pi_T)}{s^2(\Pi_L-\Pi_T)}\}. \qquad (26)
\end{aligned}
$$

To show that the above leading order (in t) cross sections give the dominant contribution, we evaluate the total and transport cross sections by using the t-channel expression for $\frac{d\sigma}{dt}$ as given by Eq.(20) and then plot the differences between the full and the leading order expressions for the total cross section in Fig.1. The graphs show that the difference between the full cross sections and the leading order cross sections are very small. So, for practical purposes, one can use Eq. (25) and (26) as the total and transport cross sections for the process $gg \to gg$ in the medium. In the figures we use $T = \frac{\sqrt{s}}{5.4}$ and $\alpha = 0.3$.

The importance of the medium modified total and transport cross sections given in Eq. (25) and (26) will be discussed below. To demonstrate it, we evaluate the total and transport cross section by using Eq. (23) which yields:

$$
(\sigma_{\rm tot})_{\rm lead.cut-off} = \int_{-\frac{s}{2}}^{0} dt\ (\frac{d\sigma}{dt})_{\rm lead.cut-off} = (\frac{9\pi\alpha^2 s}{4\Pi_L^2+2s\Pi_L}), \qquad (27)
$$

and

$$
\begin{aligned}
(\sigma_{\rm tr})_{\rm lead.cut-off} &= \int_{-\frac{s}{2}}^{0} dt\ (\frac{d\sigma}{dt})_{\rm lead.cut-off}\ \frac{4ut}{s^2} \\
&= 9\pi\alpha^2(2\frac{\ln(\frac{s}{2\Pi_L}+1)-1}{s} + 4\frac{\Pi_L\ln(\frac{s}{2\Pi_L}+1)}{s^2} - \frac{1}{s+2\Pi_L}). \qquad (28)
\end{aligned}
$$

These are the cross sections obtained by introducing a Debye screening mass by hand into the vacuum formula (see Eq. (23)). As already mentioned, there is no way that magnetic screening is incorporated in these formulas. However, one could argue that the contribution from the magnetic sector to the total and transport cross section is small. This is to be checked here. Since any significant change in the total and transport cross sections crucially influences the predictions for all the global quantities and the signatures of the quark-gluon plasma (see [4]), it is important to compare our medium modified cross section (both electric and magnetic screening taken into account) with that of the Debye screened cross sections obtained by using Eq. (23). In Fig. 2 we plot the total cross section obtained by using the medium modified propagator including electric and magnetic sreening (see Eq. (25)) and the total cross section obtained by using the in-vacuum propagator with a Debye screening mass as a cut-off (see Eq. (27)). In this figure, we use the values of s and α which correspond to a "realistic" situation at RHIC [4]. It can be seen that for the values of s and α considered here, the difference in the two cross sections increases for decreasing values of s. In Fig.3, we

plot the transport cross sections for the two cases described above (Eq.(26) and (28)). The transport cross section directly enters into the collision term (see Eq. 5) and so determines the evolution of the quark-gluon plasma. Similar to the total cross section, it can be seen that the medium modified transport cross section is enhanced in comparison to the other for smaller values of s. Hence, it can be expected that all the global quantities and the equilibration time might change when the vacuum propagator is replaced by the medium modified one. However, this has to be checked by including all these features in a self consistent transport study. For example, in the above plots, for simplicity we have used a constant value of $\alpha = 0.3$. In "realistic" situations at RHIC and LHC the α, s, total cross section, transport cross section, as well as all other quantities are time dependent and, therefore, have to be calculated via the distribution functions of the partons, which in turn are obtained by solving the transport equation self-consistently [4]. As the self-consistent transport study involves extensive additional numerical work, the results incorporating the medium modified transport cross section will be presented elsewhere.

In summary, the medium modified propagator has been used to evaluate the partonic scattering cross section for the process $gg \to gg$ in the QCD medium by performing an explicit sum over the physical gluon polarizations. A magnetic screening mass from a non-perturbative study was used to show that the medium modified cross section is finite, divergence free, and is uniquely determined. The medium modified cross sections yield different results than these obtained by artificially introducing a Debye screening mass by hand into the vacuum formulae. This implies that the medium modified scattering parton cross sections must be incorporated properly into the transport equations in order to study the production and possible equilibration of the minijet plasma at RHIC and LHC. Any change of the cross sections due to in-medium effects will crucially change the equilibration times, time evolution of the energy densities, number densities, temperatures of all degrees of freedom and hence, all predictions of signatures of the quark-gluon plasma, both at RHIC and LHC.

ACKNOWLEDGEMENTS

We thank Dirk H. Rischke, Stefan Hofmann, and Chung-Wen Kao for helpful discussions. G.C.N. would like to thank the Alexander von Humboldt Foundation and the BMBF for financial support. D.D.D. would like to thank the Graduiertenförderung des Landes Hessen for financial support.

REFERENCES

[1] Quark matter 2001. Proceedings, 15th International Conference on ultra-relativistic nucleus nucleus collisions, QM 2001, Stony Brook, January 2001.

[2] Strangeness in Quark Matter 2000, 5th International Conference on Strangeness in Quark Matter, Berkeley, California, July 2000.

[3] See, *e.g.*
L. D. McLerran and B. Svetitsky, Phys. Rev. D **24**, 450 (1981); L. McLerran, Phys. Rev. D **36**, 3291 (1987); R.V. Gavai, in *Quantum Fields on the Computer*, ed. M. Creutz, (World Scientific, 1992), p. 51; F. Karsch and E. Laermann, Rept. Prog. Phys. **56**, 1347 (1993) [hep-lat/9304010]; M. Oevers, F. Karsch, E. Laermann and P. Schmidt, Nucl. Phys. Proc. Suppl. **63**, 394 (1998) [hep-lat/9709071], Nucl. Phys. B **605**, 579 (2001) [hep-lat/0012023].

[4] G. C. Nayak, A. Dumitru, L. McLerran and W. Greiner, Nucl. Phys. A **687**, 457 (2001) [hep-ph/0001202].

[5] K. J. Eskola and K. Kajantie, Z. Phys. C **75**, 515 (1997) [nucl-th/9610015]; N. Hammon, H. Stocker and W. Greiner, Phys. Rev. C **61**, 014901 (2000) [hep-ph/9903527].

[6] T. Matsui and H. Satz, Phys. Lett. B **178**, 416 (1986).

[7] J. Rafelski and B. Muller, Phys. Rev. Lett. **48**, 1066 (1982) [Erratum-ibid. **56**, 2334 (1982)].

[8] M. Strickland, Phys. Lett. B **331**, 245 (1994).

[9] E. Shuryak and L. Xiong, Phys. Rev. Lett. **70**, 2241 (1993) [hep-ph/9301218].

[10] J. Alam, B. Sinha and S. Raha, Phys. Rept. **273**, 243 (1996).

[11] G. C. Nayak, Phys. Lett. B **442**, 427 (1998) [hep-ph/9801321].

[12] X. Wang and M. Gyulassy, Phys. Rev. D **44**, 3501 (1991); X. Wang, Phys. Rept. **280**, 287 (1997) [hep-ph/9605214].

[13] R. S. Bhalerao and G. C. Nayak, Phys. Rev. C **61**, 054907 (2000) [hep-ph/9907322].

[14] L. McLerran and R. Venugopalan, Phys. Rev. D **49**, 2233 (1994) [hep-ph/9309289].

[15] Y. V. Kovchegov and A. H. Mueller, Nucl. Phys. B **529**, 451 (1998) [hep-ph/9802440]; A. H. Mueller, Nucl. Phys. B **572**, 227 (2000) [hep-ph/9906322].

[16] C. D. Roberts and S. M. Schmidt, Prog. Part. Nucl. Phys. **45S1**, 1 (2000) [nucl-th/0005064].

[17] Y. Kluger, J. M. Eisenberg, B. Svetitsky, F. Cooper and E. Mottola, Phys. Rev. Lett. **67**, 2427 (1991); F. Cooper, J. M. Eisenberg, Y. Kluger, E. Mottola and B. Svetitsky, Phys. Rev. D **48**, 190 (1993) [hep-ph/9212206]; J. M. Eisenberg and G. Kaelbermann, Phys. Rev. D **37**, 1197 (1988); T. S. Biro, H. B. Nielsen and J. Knoll, Nucl. Phys. B **245**, 449 (1984); M. Herrmann and J. Knoll, Phys. Lett. B **234**, 437 (1990), D. Boyanovsky, H. J. de Vega, R. Holman, D. S. Lee and A. Singh, Phys. Rev. D **51**, 4419 (1995) [hep-ph/9408214]; H. Gies, Phys. Rev. D **61**, 085021 (2000) [hep-ph/9909500].

[18] K. Geiger and J. I. Kapusta, Phys. Rev. D **47**, 4905 (1993).

[19] K. Geiger, Phys. Rept. **258**, 237 (1995).

[20] A. Hosoya and K. Kajantie, Nucl. Phys. B **250**, 666 (1985).

[21] M. Gyulassy, Y. Pang and B. Zhang, Nucl. Phys. A **626**, 999 (1997) [nucl-th/9709025]; B. Zhang, Comput. Phys. Commun. **109**, 193 (1998) [nucl-th/9709009].

[22] P. Danielewicz and M. Gyulassy, Phys. Rev. D **31**, 53 (1985).

[23] H. A. Weldon, Phys. Rev. D **26**, 1394 (1982).

[24] P. V. Landshoff and A. Rebhan, Nucl. Phys. B **383**, 607 (1992) [Erratum-ibid. B **406**, 517 (1992)] [hep-ph/9205235].
[25] R. Cutler and D. Sivers, Phys. Rev. D **17**, 196 (1978).
[26] B. L. Combridge, J. Kripfganz and J. Ranft, Phys. Lett. B **70**, 234 (1977).
[27] T. S. Biro and B. Muller, Nucl. Phys. A **561**, 477 (1993) [nucl-th/9211011].
[28] H. Heiselberg and X. Wang, Nucl. Phys. B **462**, 389 (1996) [hep-ph/9601247].

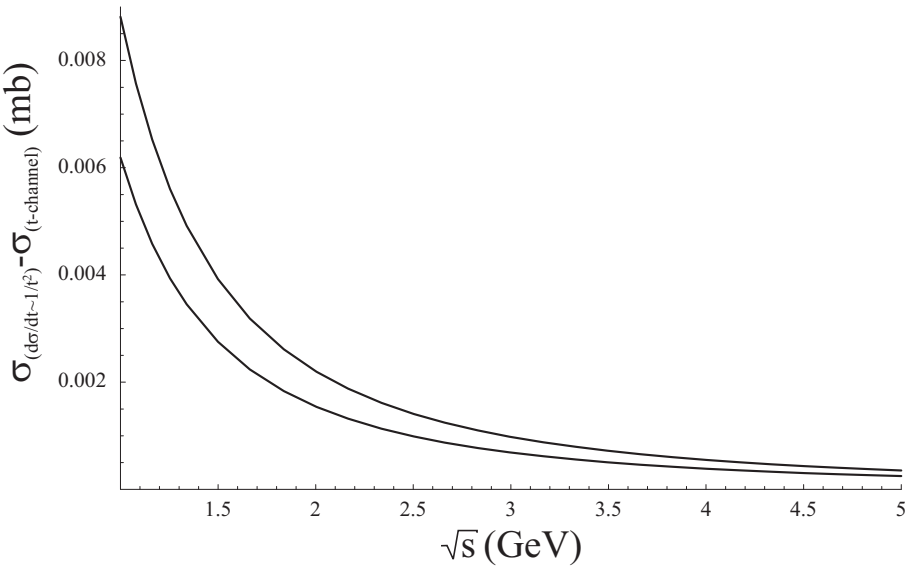

Fig. 1 In the upper curve the difference of the total cross section in small angle approximation to the same quantity obtained by using the t-channel matrix element $|\sigma_{(\frac{d\sigma}{dt}\propto\frac{1}{t^2})} - \sigma_{(\mathrm{t-channel})}|$is plotted as a function of $\sqrt{s}$ ($\alpha = 0.3$). The lower curve is the difference obtained for the transport cross sections.

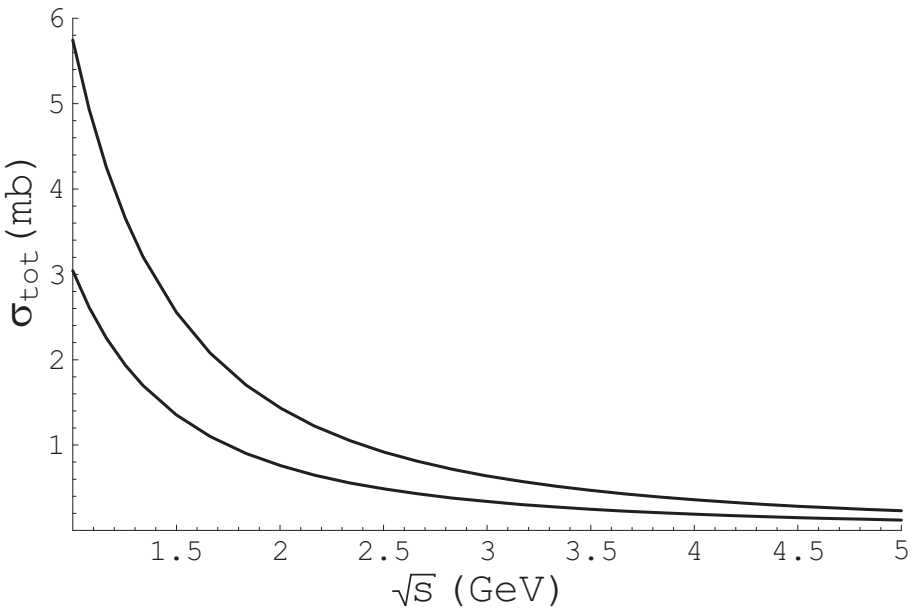

Fig. 2 The total in-medium cross section and the total cross section regularized by putting a cut-off by hand $\sigma_{\rm tot}$ is plotted as a function of $\sqrt{s}$. ($\alpha = 0.3$) The first is significantly enhanced in comparison to the second.

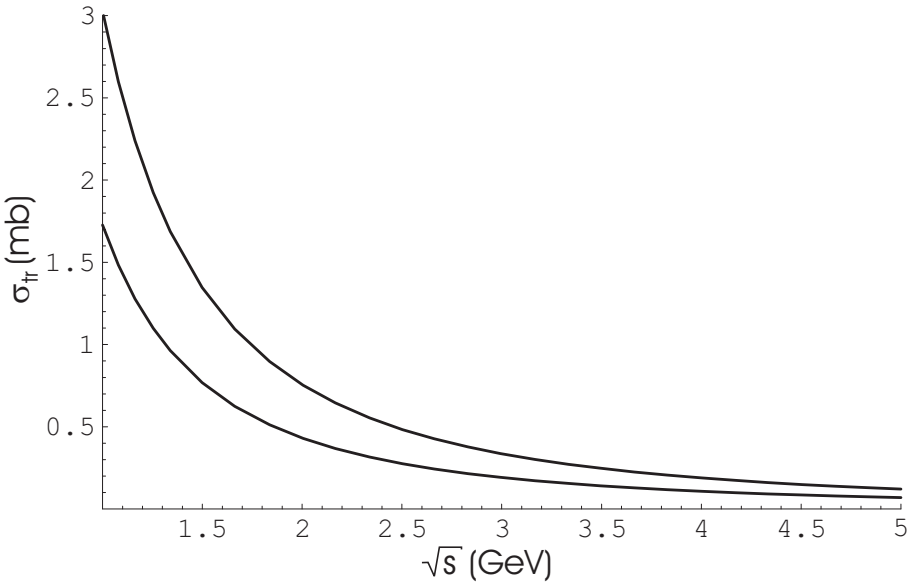

Fig. 3 The in-medium transport cross section and the transport cross section regularized by putting a cut-off by hand $\sigma_{\rm trans}$ is plotted as a function of $\sqrt{s}$.($\alpha = 0.3$) The first is significantly enhanced in comparison to the second.